

## Spiro Oligothiophenes

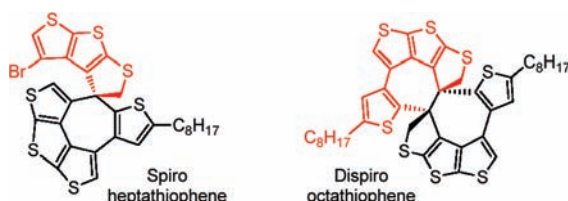
Makoto Miyasaka,<sup>†</sup> Maren Pink,<sup>‡</sup> Suchada Rajca,<sup>†</sup> and Andrzej Rajca<sup>\*†</sup>

Department of Chemistry, University of Nebraska, Lincoln, Nebraska 68588-0304, and IUMSC, Department of Chemistry, Indiana University, Bloomington, Indiana 47405-7102

arajca1@unl.edu

Received May 20, 2010

## ABSTRACT



Linear oligothiophenes, containing annelated dithieno[2,3-*b*:3',2'-*d*]thiophene units, undergo unexpected spirocyclizations upon treatment with trifluoroacetic acid. The resultant spiro oligothiophenes possess novel structures in which the spiro or dispiro skeleton is within an all-thiophene/dihydrothiophene framework. Racemic dispiro octathiophene is obtained with high diastereoselectivity and in high yield.

Oligothiophenes are a promising class of  $\pi$ -conjugated materials for advanced technological applications.<sup>1</sup> To date, linear oligothiophenes are the most widely studied, though those with novel molecular topologies have been explored in the search for materials and devices with enhanced properties. In particular, oligothiophenes with unique three-dimensional (3D) structures are of interest in the development of organic electronics.<sup>2</sup> Some examples of such structures include carbon–sulfur [*n*]helicenes with chiral  $\pi$ -systems,<sup>3–9</sup> as well as dendritic<sup>10,11</sup> and tetrahedral oligothiophenes.<sup>12</sup>

The spirocyclic skeleton is among the few effective molecular frameworks for 3D structures. Spiro compounds are promising for optoelectronic applications, in part due to their propensity to form stable amorphous materials with high glass transition temperatures.<sup>13</sup> Notably, most of these spiro compounds are based on the spirobifluorene core, which serves as a scaffold for connecting two extended  $\pi$ -systems via an sp<sup>3</sup>-hybridized atom.<sup>13–17</sup> Recently, some new spirofluorene derivatives such as heteroarene-fused dispiro compounds and dispiroanthene–indenofluorene have been reported.<sup>18</sup>

Herein we disclose new spiro oligothiophenes **1** and **2**, in which the spiro or dispiro skeleton is incorporated within

<sup>†</sup> University of Nebraska.<sup>‡</sup> Indiana University.(1) Mishra, A.; Ma, C.-Q.; Bäuerle, P. *Chem. Rev.* **2009**, *109*, 1141–1276.(2) Roncali, J.; Leriche, P.; Cravino, A. *Adv. Mater.* **2007**, *19*, 2045–2060.(3) (a) Rajca, A.; Miyasaka, M.; Pink, M.; Wang, H.; Rajca, S. *J. Am. Chem. Soc.* **2004**, *126*, 15211–15222. (b) Rajca, A.; Wang, H.; Pink, M.; Rajca, S. *Angew. Chem., Int. Ed.* **2000**, *39*, 4481–4483.(4) Miyasaka, M.; Rajca, A.; Pink, M.; Rajca, S. *J. Am. Chem. Soc.* **2005**, *127*, 13806–13807.(5) Rajca, A.; Rajca, S.; Pink, M.; Miyasaka, M. *Synlett* **2007**, 1799–1822.(6) Miyasaka, M.; Pink, M.; Rajca, S.; Rajca, A. *Angew. Chem., Int. Ed.* **2009**, *48*, 5954–5957.(7) Li, C.; Shi, J.; Xu, L.; Wang, Y.; Cheng, Y.; Wang, H. *J. Org. Chem.* **2009**, *74*, 408–411.(8) Zak, J. K.; Miyasaka, M.; Rajca, S.; Lapkowski, M.; Rajca, A. *J. Am. Chem. Soc.* **2010**, *132*, 3246–3247.(9) Tian, Y.-H.; Park, G.; Kertesz, M. *Chem. Mater.* **2008**, *20*, 3266–3277.(10) Ma, C.-Q.; Mena-Osteritz, E.; Debaerdemaeker, T.; Wienk, M. M.; Janssen, R. A. J.; Bäuerle, P. *Angew. Chem., Int. Ed.* **2007**, *46*, 1679–1683.(11) Harpham, M. R.; Süzer, U.; Ma, C.-Q.; Bäuerle, P.; Goodson, T., III. *J. Am. Chem. Soc.* **2009**, *131*, 973–979.(12) Matsumoto, K.; Tanaka, T.; Kugo, S.; Inagaki, T.; Hirao, Y.; Kurata, H.; Kawase, T.; Kubo, T. *Chem. Asian J.* **2008**, *3*, 2024–2032.(13) Saragi, T. P. I.; Spehr, T.; Siebert, A.; Fuhrmann-Lieker, T.; Salbeck, J. *Chem. Rev.* **2007**, *107*, 1011–1065.(14) Pei, J.; Ni, J.; Zhou, X. H.; Cao, X. Y.; Lai, Y. H. *J. Org. Chem.* **2002**, *67*, 8104–8113.(15) Tour, J. M. *Chem. Rev.* **1996**, *96*, 537–554.(16) Wu, R.; Schumm, J. S.; Pearson, D. L.; Tour, J. M. *J. Org. Chem.* **1996**, *61*, 6906–6921.(17) Oligothiophenes linked through saturated spirocyclopentane and its sila-analogue are of interest in the theory of molecular electronics. (a) Aviram, A. *J. Am. Chem. Soc.* **1988**, *110*, 5687–5692. (b) Reference 16. (c) Ben-Moshe, V.; Nitzan, A.; Skourtis, S. S.; Beratan, D. N. *J. Phys. Chem. C* **2010**, *114*, 8005–8013.

an all-thiophene/dihydrothiophene structure (Figure 1). We accidentally discovered **1** in the course of the synthesis of a carbon–sulfur [9]helicene.<sup>19</sup>

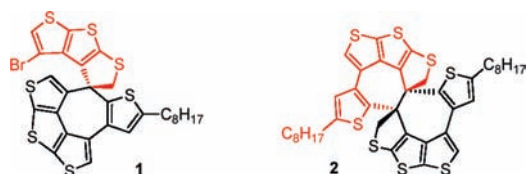
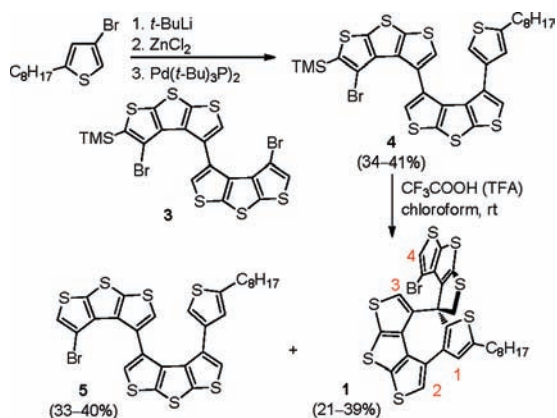


**Figure 1.** Spiro oligothiophenes.

Spiro heptathiophene **1** is formed by acid-mediated cyclization of **4**, an intermediate prepared by a Negishi cross-coupling between the  $\beta$ -positions of thiophenes<sup>20</sup> in the synthesis of [9]helicene (Scheme 1). When **4** is subjected to a TFA-mediated deprotection of TMS group, typically a high-yield step in the synthesis of thiophene-based [*n*]helicenes<sup>3,6,21,22</sup> and dithieno[2,3-*b*:3',2'-*d*]thiophenes,<sup>23</sup> <sup>1</sup>H NMR spectra of the crude products showed approximately 1:1 mixtures of the deprotected heptathiophene **5** and an unexpected constitutional isomer, spiro heptathiophene **1** (Figure S3, Supporting Information).

**Scheme 1.** Synthesis of Heptathiophenes **1** and **5**.<sup>a,b</sup>



<sup>a</sup> Isolated yields. <sup>b</sup> In **1**, protons H(1)–H(4) are indicated.

To further investigate this result, we carried out the reaction of heptathiophene **5** with TFA in an NMR tube, for

(18) (a) Kowada, T.; Kuwabara, T.; Ohe, K. *J. Org. Chem.* **2010**, *75*, 906–913. (b) Cocherel, N.; Poriel, C.; Vignau, L.; Bergamini, J.-F.; Rault-Berthelot, J. *Org. Lett.* **2010**, *12*, 452–455.

(19) Synthesis of the [9]helicene will be reported elsewhere.

(20) Negishi cross-coupling between  $\beta$ -positions of thiophenes: Miyasaka, M.; Rajca, A. *Synlett* **2004**, 177–181.

(21) Miyasaka, M.; Rajca, A.; Pink, M.; Rajca, S. *Chem.–Eur. J.* **2004**, *10*, 6531–6539.

(22) The exception is one of the thiophene–phenylene [7]helicenes, for which TMS deprotection with TFA gives the product in intramolecular cyclization that is quasi[8]circulene. (a) Rajca, A.; Miyasaka, M.; Pink, M.; Xiao, S.; Rajca, S.; Das, K.; Plessel, K. *J. Org. Chem.* **2009**, *74*, 7504–7513. (b) Rajca, A.; Miyasaka, M.; Xiao, S.; Boratyński, P. J.; Pink, M.; Rajca, S. *J. Org. Chem.* **2009**, *74*, 9105–9111.

(23) Miyasaka, M.; Rajca, A. *J. Org. Chem.* **2006**, *71*, 3264–3266.

which we monitored the conversion of **5** into **1** by <sup>1</sup>H NMR spectroscopy (Figure 2). The maximum **1**/**5** ratio of 1.2 is reached after about 5 h at room temperature. In a similar experiment, when **1** is treated with TFA, <sup>1</sup>H NMR spectra show gradual conversion of **1** to **5**, reaching the identical **1**/**5** ratio of 1.2 (Figure S4, Supporting Information). These experiments indicate that at room temperature **5** and **1** are in equilibrium with  $K_{eq} = 1.2$ .

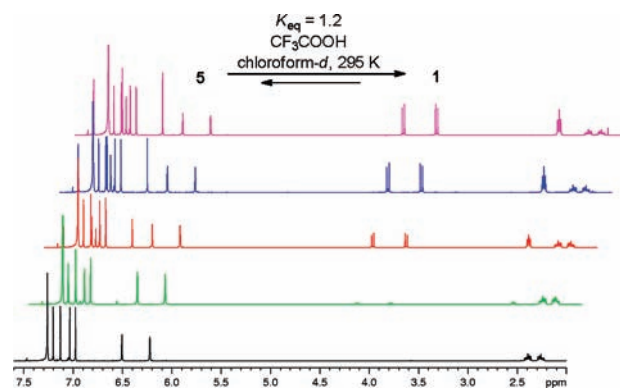
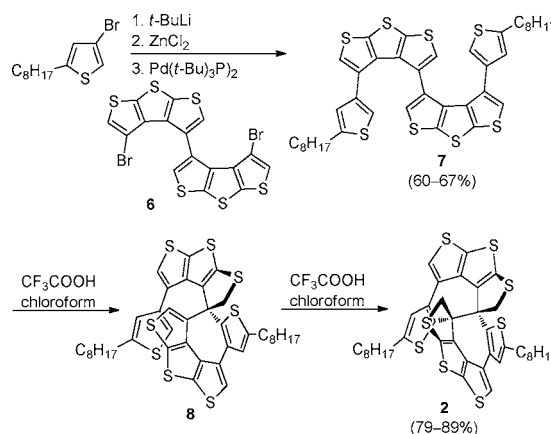


**Figure 2.** <sup>1</sup>H NMR (500 MHz, chloroform-*d*) spectra for the reaction of heptathiophene **5** with TFA. Bottom-to-top spectra taken after the following times: 0, 10, 120, 320, 1620 min.

The surprising cyclization of **4** to **1** leads us to examine acid-mediated cyclization of octathiophene **7**,<sup>4</sup> which is readily prepared by the Negishi cross-coupling as shown in Scheme 2. Treatment of **7** with TFA in chloroform at room temperature for 8 h gives a crude reaction mixture for which the <sup>1</sup>H NMR spectrum indicates that dispiro octathiophene **2** is formed in high yield and as a single diastereomer (Figure S6, Supporting Information). Interestingly, when the reaction time is shortened to 4–5 h, monospiro octathiophene **8** is detected in the crude reaction mixtures by <sup>1</sup>H NMR spectroscopy (Supporting Information).

**Scheme 2.** Synthesis of Octathiophenes **2** and **7**.<sup>a</sup>



<sup>a</sup> Isolated yields.

To gain insight into this transformation, we carried out the reaction of octathiophene **7** with TFA in an NMR tube. Monitoring of the reaction by  $^1\text{H}$  NMR spectroscopy indicates an initial rise of the spectrum corresponding to nonsymmetrical, monospiro octathiophene **8**, ultimately followed by its conversion to symmetrical dispiro octathiophene **2** (Figure 3).

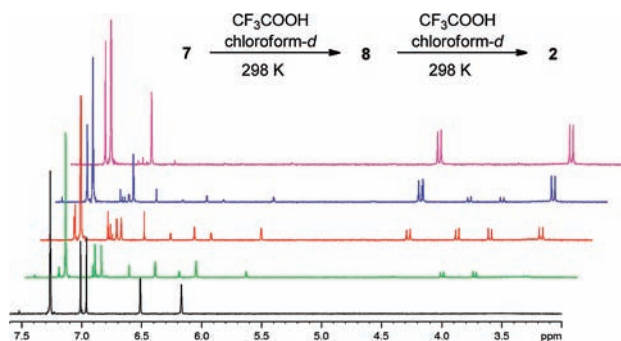


**Figure 3.**  $^1\text{H}$  NMR (400 MHz, chloroform- $d$ ) spectra for the reaction of octathiophene **7** with TFA. Bottom-to-top spectra taken after the following times: 0, 8, 40, 115, 265 min.

In a similar experiment but starting from **2**, no change in the  $^1\text{H}$  NMR spectrum of **2** in the presence of TFA was observed over a period of 18 h. These results indicate that the conversion of **7** to **2** is practically complete, thus accounting for high isolated yields of **2**.

Although **1** and **2** are difficult to crystallize, weakly diffracting, needle-shaped crystals could be grown for **1**. The X-ray structure of **1**, obtained with synchrotron radiation, qualitatively confirms spiro connectivity shown in Figure 1.<sup>24</sup>

Further evidence for connectivity and symmetry in **1** and **2** is provided by NMR spectroscopy, as well as mechanistic considerations outlined in Schemes 3 and 4. In order to assist the assignment of the NMR spectra and the understanding of formation of **1** and **2**, we compute model structures of **1** and **2**, in which the octyl chains are replaced with methyl groups, using DFT methods at the B3LYP/6-31(d,p) level of theory, e.g., **1a-R** (Scheme 3) with an (*R*)-configuration is a simplified structure for **1**.<sup>25</sup>

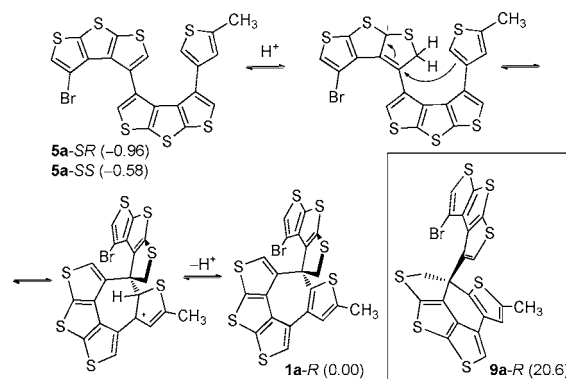
In the proposed pathway leading to **1a-R** (Scheme 3), the starting heptathiophene can exist in two nonplanar conformations, **5a-SR** and **5a-SS**, with either (*S,R*) or (*S,S*) configuration of their chiral axes; the (*S*) configuration of the chiral axis along the CC bond connecting the terthiophene units corresponds to the (*R*) configuration of the chiral center in the spiro product **1a-R**. The relative energies are within 1 kcal mol<sup>-1</sup> for **1a-R**, **5a-SR**, and **5a-SS** (Scheme 3), which is qualitatively consistent with  $K_{\text{eq}} \approx 1$  for the formation of **1** under thermodynamic control (Figure 2).<sup>26</sup>

(24) X-ray structure of **1** could only be partially refined because of small, low-quality crystals (Figure S1, Table S1, Supporting Information).

(25) Frisch, M. J. et al. *Gaussian 03, Revision E.01*; Gaussian: Wallingford, CT, 2004.

(26) Accurate free energies would require higher level of theory.

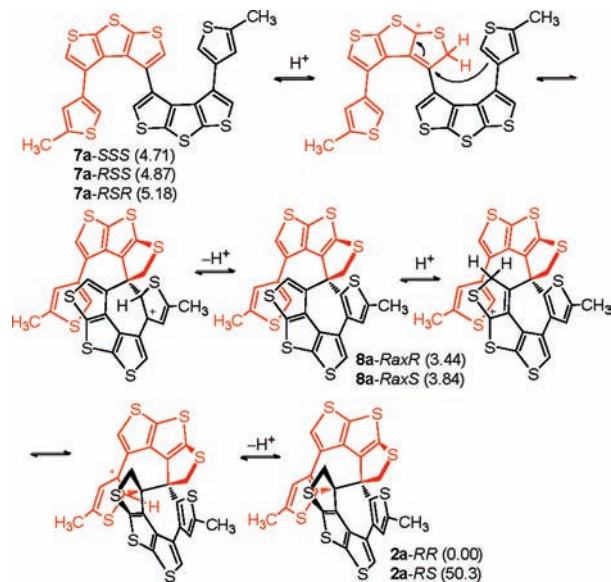
### Scheme 3. Acid-Mediated Spiro-Cyclization of Heptathiophene<sup>a</sup>



<sup>a</sup> Relative energies (kcal mol<sup>-1</sup>) at the B3LYP/6-31G(d,p) level after the ZPVE correction.

In contrast, the calculated energy for  $C_2$ -symmetric dispiro octathiophene **2a-RR** is about 5 kcal mol<sup>-1</sup> below the starting octathiophenes **7a-SSS**, **7a-RSS**, and **7a-RSR** and about 3 kcal mol<sup>-1</sup> below the intermediate spiro octathiophenes **8a-RaxR** and **8a-RaxS** (Scheme 4). Also, **2a-RR** is about 50 kcal mol<sup>-1</sup> below its  $C_1$ -symmetric *meso*-diastereomer **2a-RS**. For the reaction under thermodynamic control, these calculated energies are consistent with high conversion of **7** to **2** (Figure 3) and with perfect diastereoselection for the chiral (racemic) diastereomer of **2**.

### Scheme 4. Acid-Mediated Bis-Spiro-Cyclization of Octathiophene<sup>a</sup>



<sup>a</sup> Relative energies (kcal mol<sup>-1</sup>) at the B3LYP/6-31G(d,p) level after the ZPVE correction.

We propose that the initial step in each spirocyclization is a protonation at the  $\alpha$ -position of the terthiophene moiety to provide an allyl carbocation stabilized by two sulfur atoms

(Schemes 3 and 4).<sup>27</sup> While a few such resonance-stabilized carbocations are possible, only ones leading to the least strained 7-membered ring, via the electrophilic aromatic substitution at the  $\alpha$ -position of the alkylthiophene moiety, give the lowest energy spiro products. For example, a 6-membered ring product such as **9a-R** (Scheme 3) is about 20 kcal mol<sup>-1</sup> above **1a-R**.<sup>28</sup>

The CH<sub>2</sub> groups resulting from protonation of terthiophene moieties appear in the <sup>1</sup>H NMR spectra as AB spin systems in the 3.4–4.5 ppm range, with integration of 2 and 4 protons for **1** and **2**, respectively. Aromatic protons in **1** (Scheme 1) are assigned as follows. H(1) is identified by the resolved allylic coupling of 1 Hz and the corresponding long-range COSY cross-peak. H(2) is assigned by the H(1)–H(2) ROESY cross-peak and selective NOE that may be correlated with the DFT-calculated H $\cdots$ H distance of 2.32 Å. The DFT-calculated, through-space H $\cdots$ H distance of 3.78 Å between H(3) and the upfield diastereotopic proton of the CH<sub>2</sub>-group, is corroborated with a weak NOE on the order of 1%. H(4) does not show an NOE, which is consistent with the relatively long DFT-calculated through-space H $\cdots$ H distances to other protons, with minimum distance of 5.71 Å for H(4) $\cdots$ H(3).

Using these assignments for **1** and DFT-calculated isotropic NMR shieldings for **1a-R**, an excellent correlation ( $R^2 = 0.99$ ) is found between the calculated and experimental <sup>1</sup>H chemical shifts (Figure S28, Supporting Information).<sup>29,30</sup> Notably, this correlation is practically indistinguishable from the correlation between the calculated and experimental <sup>1</sup>H chemical shifts for C<sub>2</sub>-symmetric **2a-RR** and **2**.<sup>31</sup> These correlations confirm the structures of **1** and **2**.

UV–vis absorption spectra for **1** and **2** are in a qualitative agreement with the TD-DFT calculated spectra, including bathochromic shifts for **2** and **2a-RR** (Figure 4).

This bathochromic shift is also found in the calculated CD spectra for **1a-R** and **2a-RR** (Figure S2, Supporting Informa-

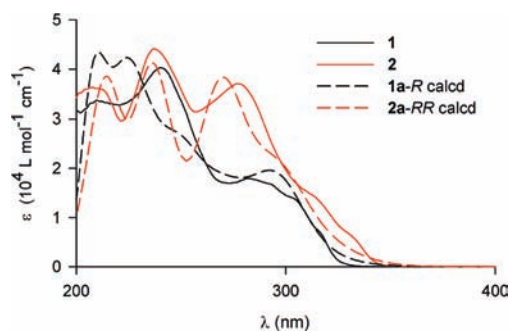


**Figure 4.** UV–vis absorption spectra for **1** and **2** in cyclohexane and spectra for **1a-R** and **2a-RR** calculated at the TD-B3LYP/6-31G(d,p)/IEF-PCM-UAHF level of theory. The calculated spectra are vertically scaled.

tion) with the calculated  $|\Delta\epsilon_{\max}| \approx 100\text{--}150\text{ L mol}^{-1}\text{ cm}^{-1}$  (Figure S2, Supporting Information) that is similar to  $|\Delta\epsilon_{\max}|$  in carbon–sulfur [*n*]helicenes.<sup>5,6</sup>

Racemic oligothiophenes **1**, **2**, **4**, and **7** possess chiral conformations on the NMR time scale of enantiomer separation indicated by well-resolved peaks resulting from diastereomeric interactions with chiral shift reagents. For **2**, well-resolved peaks resulting from diastereomeric interactions with the chiral stationary phase of the HPLC column are obtained as well (Figures S17–S27, Supporting Information).

In conclusion, novel spiro oligothiophenes in which the spiro or dispiro skeleton is within an all-thiophene/dihydrothiophene framework have been synthesized via acid-mediated spirocyclizations of linear oligothiophenes. The reaction pathways to these spiro oligothiophenes, including high diastereoselectivity for racemic dispiro octathiophene, are supported by the DFT calculations. These spiro oligothiophenes may provide a new entry to chiral oligothiophenes as new building blocks for chiral materials.

**Acknowledgment.** We thank the National Science Foundation for support of this work through Grant No. CHE-0718117. We thank Dr. Przemysław J. Boratyński (University of Nebraska) for assignments of NMR spectra.

**Supporting Information Available:** Complete acknowledgment and ref;<sup>25</sup> experimental and computational details. This material is available free of charge via the Internet at <http://pubs.acs.org>.

OL1011696

(27) Yu, Y.; Gunic, E.; Miller, L. L. *Chem. Mater.* **1995**, *7*, 255–256.

(28) An alternative seven-membered ring spiro product **10a-R** (Table S4, Supporting Information), derived from the initial protonation at  $\alpha$ -position of the monothiophene unit, is about 13 kcal mol<sup>-1</sup> above **1a-R**. We thank the reviewer for pointing out this possibility.

(29) (a) Jain, R.; Bally, T.; Rablen, P. R. *J. Org. Chem.* **2009**, *74*, 4017–4023. (b) Saielli, G.; Bagno, A. *Org. Lett.* **2009**, *11*, 1409–1412.

(30) (a) Calculations at the GIAO/B3LYP/6-31G(d,p) level using IEF-PCM-UA0 solvent model for chloroform. (b) <sup>13</sup>C resonances in **1** could only be partially assigned using HSQC and HMBC experiments; the correlation with calculated <sup>13</sup>C chemical shifts **1a-R** versus **1** gives  $R^2 = 0.95$  (Figure S28, Supporting Information).

(31) One of the calculated <sup>1</sup>H chemical shifts in the C<sub>7</sub>-symmetric **2a-RS** is about 1 ppm higher than the experimental value in **2**.